Tire and road wear particles in infiltration pond sediments: Occurrence, spatial distribution, size fractionation and correlation with metals

Tiago De Oliveira, Du Phuc Tho Dang, Maxime Chaillou, Sampriti Roy, Nadège Caubrière, Martin Guillon, Martin Guillon, David Mabilais, Sophie Ricordel, Liliane Jean-Soro, et al.

Title

Tire and road wear particles in infiltration pond sediments: Occurrence, spatial distribution, size fractionation and correlation with metals

Authors

Tiago De Oliveira[1]*, Du Phuc Tho Dang[1], Maxime Chaillou[1], Sampriti Roy[1], Nadège Caubrière[1], Martin Guillon[1], David Mabilais[1], Sophie Ricordel[1], Liliane Jean-Soro[1], Béatrice Béchet[1], Bogdan Muresan Paslaru[2], Laurence Poirier[3], Johnny Gasperi[1]

[1] Univ Gustave Eiffel, GERS-LEE, F-44344 Bouguenais, France

[2] Univ Gustave Eiffel, AME-EASE, F-44344 Bouguenais, France

[3] Nantes Université, ISOMer, F-44000 Nantes, France

*Corresponding author: T. De Oliveira, Allée des Ponts et Chaussées, F-44344 Bouguenais, France

Email address: tiago.de-oliveira@univ-eiffel.fr

Highlights

- The TRWP footprint in infiltration pond sediments is assessed by Pyr-GC-MS.
- Infiltration pond sediments are contaminated in TRWP up to 65 mg/g.
- The TRWP-metals correlation suggests TRWP's role as a metal indicator.
- Infiltration ponds prove to be efficient in retaining TRWP.

Graphical abstract

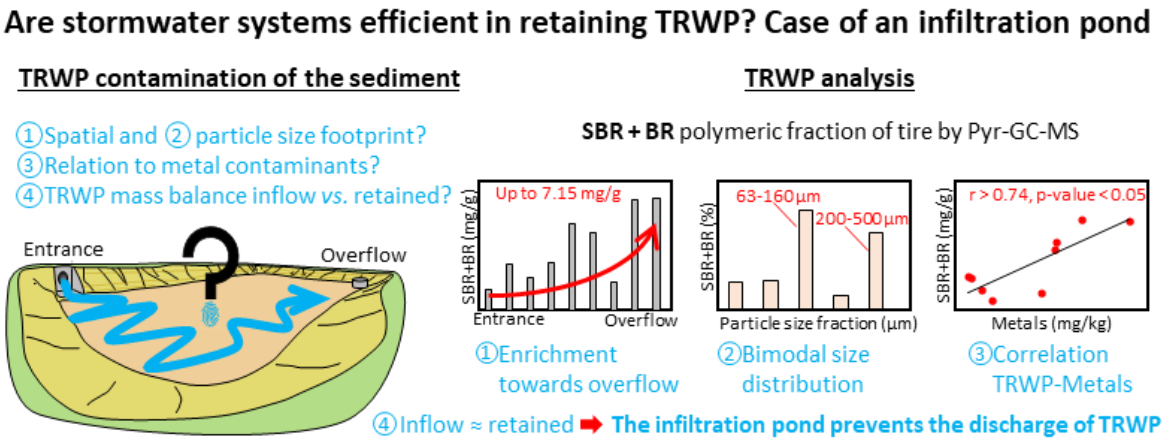

Abstract

Stormwater systems, such as infiltration ponds or basins, play a critical role in managing runoff water and reducing particulate pollution loads in downstream environments through decantation. Road runoff carries several pollutants, including trace metals and tire and road wear particles (TRWP). To improve our understanding of infiltration ponds as regards TRWP and their capacity to reduce TRWP loads, we have studied the occurrence, spatial distribution and size distribution of TRWP, as well as their relationship with metals, in considering the input of metals as tire additives, in the sediments of an infiltration pond located along the Nantes urban ring road (Western France), which happens to be a high-traffic roadway site. The sediment was analyzed using pyrolysis coupled with gas chromatography-mass spectrometry to determine the polymeric content of tires, specifically in quantifying the styrene-butadiene rubber (SBR) and butadiene rubber (BR) pyrolytic markers. By applying an SBR + BR-to-TRWP conversion factor, the results showed significant TRWP contamination, up to 65 mg/g, with a spatial enrichment from the entrance to the overflow section of the pond. Size fractionation revealed a bimodal distribution, indicating two distinct types of TRWP. The first type is characterized by small diameters (63-160 µm), suggesting the presence of TRWP less integrated with mineral and organic particles. The second type, characterized by larger diameters (200-500 µm), suggests a more pronounced integration with these same mineral and organic particles. A significant positive correlation between TRWP and metals (As, Cd, Cr, Cu, Li, Mo, Ni, Sb, V, Zn) was found ($r > 0.739$, $p < 0.05$). This correlation implies that TRWP and/or their associated phases may act as an indicator of metal contamination in the pond sediments. Lastly, a mass balance between TRWP inputs and the amount retained in the sediments underscores the role of infiltration ponds as "sinks" for TRWP.

Keywords: Stormwater management, sediment pollution, tire and road wear particles, trace metals, pyrolysis-GC-MS.

1. Introduction

At present, the literature quite frequently states that efficient stormwater management has become a major challenge. For the past several decades, Sustainable Drainage Systems (SuDS) have been implemented in sensitive areas, particularly urban ones (Wei *et al.* 2023). Within this category of stormwater management systems, among the most widespread types of infrastructure are retention and infiltration ponds or infiltration basins. Although "infiltration pond" and "infiltration basin" refer to the same infrastructure, the term "infiltration pond" will be preferred in this manuscript. These infrastructures play a critical role in not only regulating stormwater flows, in some cases allowing aquifers to be recharged, but also reducing pollutant loads into downstream environments, mostly through decantation, photooxidation or biodegradation (Dang *et al.* 2023).

The runoff collected from road surfaces contains several categories of pollutants, including metals, organic micropollutants and microplastics, most of which head towards SuDS infrastructure. Numerous studies have provided valuable insights into the presence of metals in sediment from SuDS, thereby highlighting their significant accumulation and the need for more tailored management strategies aimed at the removal of contaminated sediments (Allen *et al.* 2017; Clozel *et al.* 2006; El-Mufleh *et al.* 2014; Heal *et al.* 2006; Humphrey *et al.* 2023; Tedoldi *et al.* 2017).

More recently, studies have been increasingly focused on both macroplastics and microplastics in SuDS, in light of the evidence of their ubiquity and high load in urban runoff (García-Haba *et al.* 2023; Ledieu *et al.* 2022; Werbowski *et al*. 2021). Polyethylene, polypropylene, polyester, acrylic, polyamide and polystyrene have emerged as the most abundant polymers, typically assessed via Fourier-transform infrared spectroscopy, with concentrations ranging from a few items per kg of infiltration pond sediment to 10^6 items/kg (Koutnik *et al.* 2022). Reviews

conducted by García-Haba *et al.* (2023) and Österlund *et al.* (2023) on this topic suggest that SuDS effectively mitigate, by means of decantation, the release of microplastics to downstream environments, thus acting as sinks for these materials.

Studies performed on infiltration ponds with respect to metal contaminants were found to be well documented compared to the studies on macroplastic and microplastic particles. Within the microplastic category and considering that elastomers are included in the definition of microplastics, tire and road wear particles (TRWP) have been, until recently, even less extensively studied. TRWP are formed by the aggregation of tire particles (mainly constituted by a polymeric fraction of styrene-butadiene rubber (SBR) and butadiene rubber (BR)) and abraded road materials, which are recognized as a major source and pathway for microplastics into the environment (Kole *et al.* 2017). These "heteroaggregates" are being continuously generated by road traffic, with an estimated annual mass emission per capita ranging from 0.2 to 5.5 kg (Baensch-Baltruschat *et al.* 2020). More specifically, the majority of the emitted TRWP (i.e. > 99%) occurs at the road surface, with a dispersion primarily ascribed to runoff into the environment (De Oliveira *et al.* 2024).

Consequently, road dust is highly concentrated in TRWP, hence leading to prolonged impregnation of soils and sediments in the proximity of highways and roads within urban areas. Such areas are characterized by TRWP concentrations ranging from a few to hundreds of grams of TRWP per kilogram of soil or sediment matrices (Eisentraut *et al.* 2018; Federico *et al.* 2023; Goßmann *et al.* 2021; Mengistu *et al.* 2021; Rødland *et al.* 2022; Unice *et al.* 2012). Given the occurrence of TRWP in the urban environment, their presence raises considerable concerns for several reasons, including: i) the simultaneous diffusion of a hazardous mix into diverse environmental compartments (Järlskog *et al.* 2022; Zhu *et al.* 2024); ii) the ecotoxicological effects of the many additives and other compounds constituting TRWP, encompassing both organic and inorganic additives, which have been identified as highly toxic to organisms

(Capolupo *et al.* 2020; Dudefoi *et al.* 2024; Jiang *et al.* 2023; Li *et al.* 2024; Müller *et al.* 2022; Page *et al.* 2022; Peng *et al.* 2022; Roubeau Dumont *et al.* 2023; Tian *et al.* 2021; Yang *et al.* 2022); and iii) the lack of a quantitative understanding of TRWP aging processes, with the release of chemicals through leachate over time (Wagner *et al.* 2022).

Up until now, only a few studies have assessed the occurrence of TRWP within the sediment of the most strategic and widespread urban infrastructure; moreover, they have revealed an accumulation ranging up to hundreds of milligrams of TRWP per gram of dried sediment (Eisentraut *et al.* 2018; Gaggini *et al.* 2024; Klöckner *et al.* 2019; Ziajahromi *et al.* 2023). However, none of these studies has ever evaluated the effectiveness of stormwater systems in reducing TRWP contamination or actually proposed some keys to managing the contaminated sediments. If sediment management and its removal were to be neglected, then the intended purpose of SuDS would become obsolete, in potentially transforming the SuDS from sinks into sources of pollution (Humphrey *et al.* 2023). Hence, understanding the quality of sediments becomes imperative to optimizing the operational efficiency of SuDS (Färm, 2002).

To gain new insight into the fate of TRWP within infiltration ponds and infiltration ponds' ability to reduce the TRWP discharge into aquatic ecosystems, we have explored herein for the very first time: i) the contamination footprint of TRWP (including occurrence, spatial distribution and particle size fractionation) within the sediment of an infiltration pond located near the Nantes urban ring road (Western France); ii) the relationship between TRWP and metals, since metals are used as tire additives and may also originate from other vehicular and road wear sources, thus suggesting that TRWP may act as a pathway for metal pollution; and iii) the role of an infiltration pond in mitigating TRWP contamination by assessing the mass balance between TRWP inputs and the amount retained in the sediments. Our analysis has focused on the synthetic rubber content of tires (specifically SBR and BR) by using pyrolysis coupled with gas chromatography-mass spectrometry (Pyr-GC-MS). On the whole, we are

expecting that the data acquired will contribute to improving those management practices aimed at reducing pollutant discharge into the downstream environment.

2. Materials and Methods

2.1 Sampling site

The studied site is an infiltration pond (Fig. 1), located in the city of Nantes (Western France, 47°11’05’’N, 1°36’51’’W), designed to receive runoff from the southern section of the Cheviré Bridge (location of the infiltration pond is available in the Appendix, Figures SI-1). This section encompasses 0.8 km of the total 1.6 km length of the bridge, covering a drainage area of 2.2 ha of impervious asphalt. The Cheviré Bridge is a component of the N844 ring road crossing the Loire River characterized by: three lanes in both directions, a 70 km/h speed limitation, and the capacity to carry heavy traffic with an annual traffic count reaching approximately 100,000 vehicles per day in 2019, of which 10% were heavy vehicles (Dang *et al.* 2023). The average daily traffic during the study period, from July 2020 to March 2021, was measured at 88,500 vehicles. The pond's unique drainage surface and design make it exceptionally well suited for a case study focusing on road runoff assessment.

Figure 1: Photograph of the studied infiltration pond. The inlet is located on the left side of the pond. A close-up of the overflow is shown in the bottom right corner.

The runoff drainage system includes zinc gutters, polyvinyl chloride pipes and concrete pipes, all of which facilitate the transport of runoff from the bridge to the infiltration pond. The pond was commissioned in April 1991, at the same time as the bridge. Over the years, the accumulation of sediment and the proliferation of dense vegetation prompted the first complete cleaning of the pond on July 21, 2020. The sediment deposit covers an area of 610 m^2. The substrate beneath the pond sediments is mainly composed of silty sand, over the first 4 meters, and clay-silt sand alluvium from 4 to 30 meters.

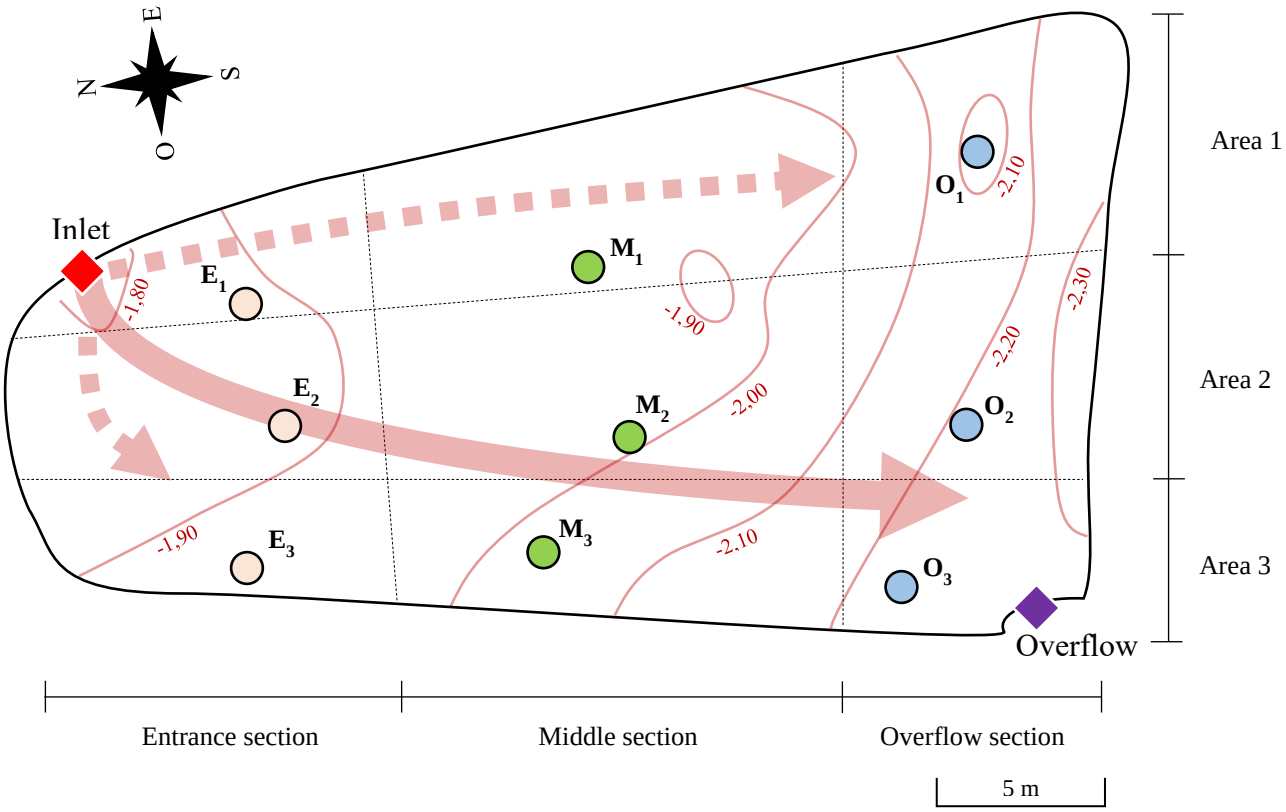

Figure 2: Location of the sampling points and topography of the infiltration pond. The topography is represented by the light red lines. Values are expressed in meters, with the reference level located at the soil surface. The surface of the pond was divided into three sections (entrance, middle, overflow) and three areas (1, 2, 3). The inlet is positioned in the top left part of the pond, while the overflow is located at the bottom right. The solid-line arrow represents the primary runoff path from the inlet during light to moderate rain events, and the dotted arrows indicate the secondary path during heavy rain events. The primary and secondary flow paths were identified through in situ observations. The first sections impacted by rain events are the overflow and middle sections, in areas 2 and 3, followed by the entrance section and area 1.

The absence of an impermeable layer at the pond's bottom makes it permeable to runoff, thus enabling relatively rapid infiltration. The pond typically empties within 2 to 4 days into the substratum (El-Mufleh *et al.* 2014). However, in cases where the runoff volume surpasses the pond's capacity, a downstream overflow facilitates the direct discharge of excess water into the Loire River. The flow of runoff into the infiltration pond, and consequently its filling, is influenced by both the topography and the intensity and duration of rainfall events (Fig. 2).

2.2 Sediment sampling

The sampling step was conducted on March 25, 2021 when the pond was dry, following an 8-month period of sediment accumulation within the infiltration pond. The pond's surface was delineated into three sections: entrance, middle, and overflow, with further division into three specific areas (Fig. 2). The sediment layer thickness was measured at approximately 1 cm within the entrance section and 2 cm within the overflow section. Pond depth was found to be -1.80 m at the entrance and -2.30 m at the overflow. The sediment samples were collected at random from a surface area measuring 33 x 35 cm at a depth corresponding to the sediment thickness (i.e. 1 to 2 cm) for each defined sampling point, in utilizing a stainless-steel hand shovel. Subsequently, the sediments were air-dried and stored in polyethylene bottles.

2.3 Metals and their physicochemical analysis

The samples designated for metals, grain size distribution and organic matter content analysis underwent a pretreatment protocol in accordance with the ISO 11464 (2006) Standard. The dried samples were sieved using a 2-mm nylon sieve. For the metals analysis, the samples were subjected to grinding and dissolution processes, as specified in the ISO 14869-1 (2001) Standard. 0.5 g of the ground sediment were calcinated at 450°C. Subsequently, 10 mL of HF (47-51%) and 3.5 mL of $HClO_4$ (65%) were added. The resulting suspension was heated at 160°C until complete evaporation. After cooling, the dry residue was exposed to 1 mL of HNO_3

for 30 minutes, followed by the addition of 20 mL of ultra-pure water. The mixture was then heated again at 80°C for 1 hour. After a second cooling, the mineralized solution was transferred to a 100-mL glass volumetric flask through a Whatman No. 40 filter. The solutions were stored in polyethylene flasks in a refrigerator at 4°C before analysis.

The analysis was conducted using inductively coupled plasma-mass spectrometry and optical emission spectroscopy, with the 8900 Triple Quadrupole from Agilent Technologies, Inc. (California, USA) and the 720-ES from Varian, Inc. (parent company: Agilent Technologies, Inc.). The samples underwent triplicate analysis, in targeting: arsenic (As), cadmium (Cd), chromium (Cr), copper (Cu), lithium (Li), molybdenum (Mo), nickel (Ni), antimony (Sb), vanadium (V), and zinc (Zn) elements in accordance with the ISO 11885 (2007) Standard (further details regarding the limits of quantification are provided in Table SI-1). An enrichment factor (EF) was calculated according to both Equation 1 and the thresholds (i.e. minor EF 1-3, moderate EF 3-5, moderate-severe EF 5-10, severe EF 10-25, very severe EF 25-50 and extremely severe EF > 50) proposed in the Rødland *et al.* study (2023).

Equation 1: $$EF = \frac{M_s}{M_b}$$

where M_s denotes the concentration of the targeted metal element M analyzed in the sample from the infiltration pond sediment, in mg/kg, and M_b the concentration of element M corresponding to the value of the geochemical background obtained from a sample extracted from the edge of the infiltration pond, in mg/kg.

A sediment granulometry assessment was performed using a Mastersizer 3000 from Malvern Panalytical (Palaiseau, France); these results are presented with respect to the median diameter (d_{50}). The organic matter (OM) content was assessed as per the EN 15935 (2021) Standard, with these results being expressed in percentage terms. In addition, exploratory scanning electron microscopy (SEM) analyses were performed on the infiltration pond sediment to

provide more detailed information on the heteroaggregates, comprising TRWP and metal components. The analyses were performed using an SU5000 microscope from Hitachi Energy (Zurich, Switzerland) in combination with an X-Flash detector 4010 from Bruker Nano (Berlin, Germany) for energy dispersive X-ray spectroscopy (SEM-EDX).

2.4 TRWP analysis

Prior to conducting the Pyr-GC-MS analysis, raw samples were dried at 105°C for 24 hours, in following the recommendations found in ISO 7270-1 (2017), and then sieved at 500 µm using a stainless-steel sieve to remove the large items. For the size fractionation analysis, the samples were fractioned by means of vibratory sieve separation on dry sediment into five fractions between < 36 µm and 500 µm (i.e. < 36, 36-63, 63-160, 160-200, 200-500 µm) using the Analysette 3 SPARTAN from FRITSCH (Idar-Oberstein, Germany). The samples were stored in calcinated glass vials at room temperature. The Pyr-GC-MS analyses were then conducted using a multi-shot pyrolyzer EGA/PY-3030D, equipped with an auto-shot sampler (AS-1020E) from FrontierLab (Fukushima, Japan). The pyrolyzer, set at 600°C, was coupled with the 8890 gas chromatography and the 5977B mass spectrometer from Agilent Technologies, Inc. (California, USA). More detailed information is provided in Table SI-2.

For the quantification of SBR and BR in the sediment samples, two specific pyrolysis products, namely 4-vinylcyclohexene (4-VCH) and 4-phenylcyclohexene (4-PCH), were selected according to our method, as presented in De Oliveira *et al.* (2024). The quantification of 4-VCH and 4-PCH was based on m/z = 54 and 104 Da, respectively. Methodological details, including preparation of the standard SBR solution in $CHCl_3$, preparation and use of the d-SBR solution as an internal deuterated standard, calibration curve, establishment of the SBR/d-SBR ratio for quantification along with information on the repeatability of standard solutions, can be found in the referenced study (De Oliveira *et al.* 2024). The analysis of multiple specific blanks (i.e.

no cup, cup only, cup + $CHCl_3$, cup + SiO_2) showed no SBR or BR contamination. The correlation coefficient of the calibration line equaled 0.998, while the limit of quantification was determined to be 5 µg SBR/g. Approximately 3 mg of sediment were weighed in pyrolysis cups using the Mettler Toledo AB265-S/FACT balance and a stainless-steel spatula.

Also, 1.27 µg of the internal standard d-SBR in solution were introduced into each cup along with the sediment sample. All samples underwent triplicate analysis, with a signal-to-noise ratio of both targeted markers exceeding 10 and a variability of less than 9%. The variability of the internal standards markers was calculated at 7%. Three control samples (i.e. 1.10 µg SBR + 2.50 mg SiO_2) were analyzed within the sediment sample sequence. The recovery calculation yielded 94 ± 8%. Results in this study are expressed in terms of mass of SBR + BR or TRWP per mass of dry sediment. The latter parameter is obtained using a median SBR + BR-to-TRWP conversion factor of 9.12, which encompasses both the minimum and maximum of mineral encrustment and SBR content in TRWP (Kreider *et al.* 2010; Rauert *et al.* 2021; Sommer *et al.* 2018; Unice *et al*. 2012).

Furthermore, the pond's theoretical effectiveness in retaining TRWP was evaluated by estimating both the inflow of TRWP into the pond and the total amount retained in the sediment using Equations 2 and 3, respectively.

Equation 2: $$TRWP_{inflow} = TWL \times W \times T \times t \times d$$

where $TRWP_{inflow}$ represents the inflow of TRWP (mg) into the pond for the considered period. TWL represents the driving wheel rate of the tire weight loss specific to the ring road that is connected to the infiltration pond (mg/km). W denotes the driving wheel contribution factor to the emission that accounts for all tires on a vehicle. Also, T is the traffic density (vehicle/day), t the time frame considered for the study (days), and d the drained road distance of the southern section of Cheviré's bridge connected to the infiltration pond (km).

Equation 3: $$TRWP_{retained} = (SBR + BR) \times C_f \times S \times Th \times \rho$$

where $TRWP_{retained}$ represents the amount of TRWP (mg) retained in the sediment of the infiltration pond. $SBR + BR$ represents the concentration of the synthetic SBR and BR polymers quantified within the sediment at each sampling point (mg/g). Moreover, C_f is the mean SBR + BR-to-TRWP conversion factor of 9.12, as obtained from the literature (Klöckner *et al.* 2021; Kreider *et al.* 2010; Rauert *et al.* 2021; Sommer *et al.* 2018; Unice *et al.* 2012); S the surface area of the considered section (m²); Th the thickness of the sediment layer of the considered section (m); and ρ the sediment density (g/cm^3) (Table SI 3 summarizes all these data).

2.5 Statistical analysis

A statistical analysis of the data was performed using Microsoft Office Excel with the XLSTAT add-on and PAST, version 4.03. The assumption of a normal data distribution was assessed by means of the Shapiro-Wilk test. Additionally, Quantile-Quantile plots were employed to provide a qualitative visual assessment of the data. Both Pearson correlation coefficients and Spearman's rank correlation coefficients were calculated in order to assess the relationships between SBR + BR, OM and the metals variables, at a confidence level of 95%. The statistical significance p-value was set at 0.05.

3. Results and Discussion

3.1 Occurrence and spatial distribution of SBR + BR

The amount of observed SBR + BR ranges from 1.28 ± 0.05 mg/g at the entrance section (sample E_1) to 7.15 ± 0.29 mg/g at the overflow section (sample O_3) (Fig. 3). The median concentration calculated for the pond equals 2.99 ± 0.12 mg/g. These values are of the same order of magnitude as those found by Eisentraut *et al.* (2018), i.e. 9.2 mg/g of SBR from

sediment samples of a treatment system for highway street runoff. When converted to TRWP concentration, our data indicate that the sediment contains up to 65.21 ± 2.64 mg of TRWP per gram. This measurement aligns, to a certain extent, with the findings of Klöckner *et al.* (2019), who reported 130 ± 15 mg of TRWP per gram found in sediment from a highway runoff treatment facility. The discrepancy between our results and those of Klöckner *et al.* can be attributed to a higher dilution of TRWP levels within the sediment of the Cheviré pond as well as the traffic volume: the highway in their study experienced 1.9 times greater vehicle flow than the ring road investigated herein. Let's note that this increased traffic correlates with a TRWP concentration twice as high.

Results revealed differential concentrations across the sections, in reflecting the specific spatial distribution of SBR + BR within the pond. Median SBR + BR concentrations per section were calculated to be: 2.06 ± 0.07, 4.99 ± 0.21 and 7.05 ± 0.29 mg/g for the entrance, middle and overflow sections respectively, thus representing a 3.4-fold increase from entrance to overflow. The variations in concentration are not only observed between different sections but also within the same section. More specifically, the enrichment levels of SBR + BR in areas 2 and 3 were on average 2.45 times higher than those in area 1 across all pond sections, which would suggest that samples from areas 2 and 3 were likely positioned near or at the main inflow of runoff from the inlet and thus closer to or at the main sediment accumulation zone. As a result, area 1 across all sections, by virtue of lying further from the source of road dust runoff, exhibits lower concentrations of SBR + BR.

To further refine the spatial distribution of SBR + BR and better understand their variability, the pond's topography was examined as a potential explanatory factor. Topography is key to shaping the sedimentary dynamics of a pond. The topographic analysis revealed a gradual increase in depth from the entrance to the overflow section, with recorded depths of -1.80 m and -2.30 m, respectively.

This deepening suggests a greater accumulation of materials within the overflow section. The sediment thickness aligns with the depth gradient, starting at approximately 1 cm in the entrance section, increasing to approx. 2 cm in the overflow section, where water covers the sediment for several days after rain events. The pond's topography and morphology influences both the orientation and directional flow of runoff within the pond and moreover promotes the accumulation and settling of TRWP in areas 2 and 3, specifically in the middle and overflow sections, along the depth gradient. This assertion is corroborated by the findings for SBR + BR. Also, the settling velocity of particles, which depends on their granulometry, plays a role in the specific spatial distribution of SBR + BR and will be further discussed below.

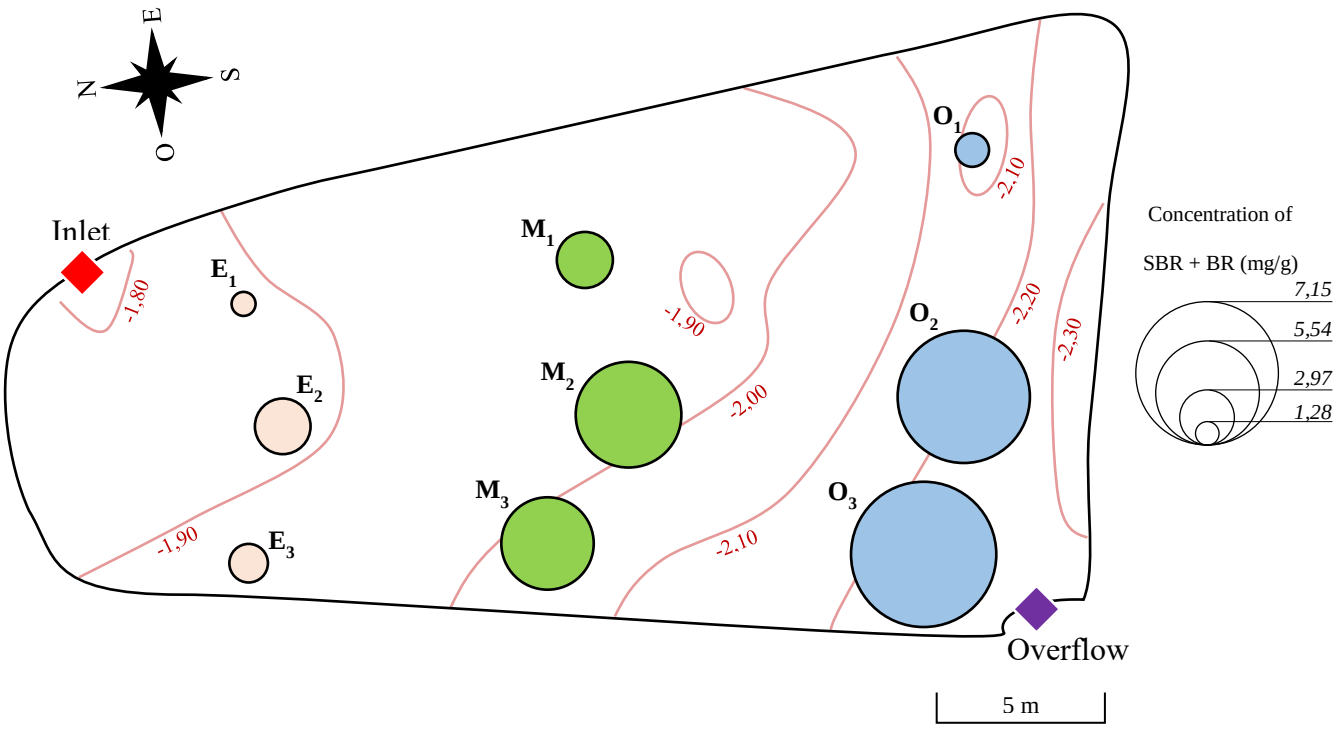

Figure 3: Spatial distribution of the SBR + BR (median of replicates, in mg/g), as quantified in sediment samples (< 500 µm) from the entrance (E_1, E_2, E_3 in orange), middle (M_1, M_2, M_3 in green) and overflow (O_1, O_2, O_3 in blue) sections, along with the topography (light red lines, values expressed in meters). The size of the circles is proportional to the amount of SBR + BR quantified in the sediments (a histogram representation of these results with error bars is provided in the Appendix, Figure SI-2).

3.2 Size fractionation of SBR + BR

The granulometry of the sediment and the size fractionation of SBR + BR content within the sediment are two parameters critical to understanding both the fate and spatial distribution of TRWP. A finer sediment was observed towards the overflow sections. The results of d_{50} averaged 104 ± 8, 83 ± 16 and 70 ± 18 µm at the entrance, middle and overflow sections, respectively (Table SI-4). The granulometric dynamic can be attributed to two factors: i) the inherent faster settling velocity of coarser particles at the inlet compared to finer particles; and ii) the turbulence generated at the inlet by the inflow of runoff water, a phenomenon that varies with rainfall intensity. The high turbulence conditions promote the remobilization of finer materials, which are subsequently transported and deposited further in the middle and overflow sections along the topography, while insufficiently affecting the transport of coarser materials, which primarily settle in the entrance section (Clozel *et al.* 2006). This effect ultimately leads to an enrichment of sands and gravels in the vicinity of the inlet, whereas finer particles become more prevalent towards the overflow section (Färm, 2002; German and Svensson, 2005).

As regards the SBR + BR content, the grain size distribution would suggest that TRWP are characterized by a finer granulometry in the overflow section, which is corroborated by a significant negative Pearson correlation coefficient between SBR + BR and d_{50} equal to -0.910 ($p < 0.05$). The analysis of SBR + BR mass proportions within each sediment size fraction, spanning from < 36 µm to 500 µm, extracted from the entrance, middle and overflow sections has confirmed the evolution in d_{50} (Fig. 4). The data also reveal a trend similar to that of the size fraction distribution of the sediments (Fig. SI 3). Comparing the finer sediment fraction (i.e. < 63 µm) from the entrance section to that of the overflow section reveals an increase in the SBR + BR mass proportion.

More specifically, in the sediment size fraction below 36 µm, the proportion rose from 11% to 19%, and in the 36-63 µm size fraction, the increase was from 12% to 18%, thus suggesting an enrichment of the sediment with TRWP within a relatively similar size range (i.e. < 63 µm). Conversely, for all sediment size fractions larger than 63 µm, a decrease was recorded in the mass proportion of SBR + BR towards the overflow section, as a result of the granulometric dynamic discussed previously.

A closer examination of the size distribution reveals a similar pattern across all three sections, which can be characterized by a bimodal distribution. The first mode, and the most prevalent fraction, was centered around 63-160 µm with a SBR + BR mass proportion of 40 ± 2%, 35 ± 2% and 33 ± 2% for the entrance, middle and overflow sections, while the second mode was centered at 200-500 µm with a SBR + BR mass proportion of 31 ± 2%, 17 ± 1% and 27 ± 2% for the entrance, middle and overflow sections. Interestingly, the first mode aligns with the size distribution of tire wear particles generated by a laboratory-scale model that simulates non-exhaust emissions, as reported by Kreider *et al.* (2010), ranging from 5 to 250 µm and displaying a unimodal distribution centered at 100 µm. Note that Kovochich *et al.* (2021) reported a similar distribution with an average TRWP size of 94 µm in tunnel dust samples. In contrast however, they observed a coarser TRWP distribution, averaging 506 µm in the sediment sample. The shift towards larger sizes observed in the tunnel dust samples, compared to TRWP within sediment samples, was attributed by the authors to the aging process, which includes aggregation with other environmental particles, such as minerals.

This process was assumed to be limited in tunnel dust but predominant in the sediment. Therefore, the bimodal distribution observed in our study may signify the presence of two distinct types of TRWP. The first and most predominant one is characterized by a smaller TRWP size and/or TRWP associated with a smaller sediment particle size, hence suggesting less aged and aggregated tire wear particles with a mineral fraction and, ultimately, with organic

phases within the sediment. The second type results in an association with the formation of larger heteroaggregates, featuring a higher mineral encrustation and thus falling in the coarser fraction of 200-500 µm.

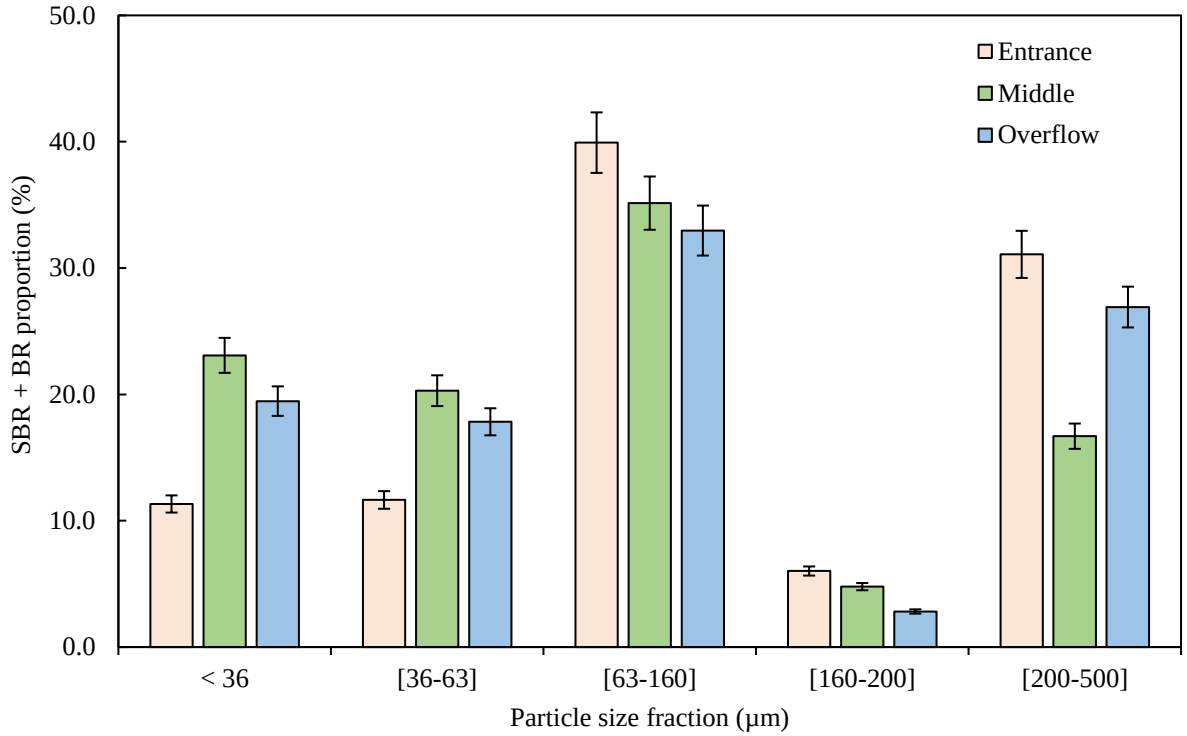

Figure 4: Mass proportion of SBR + BR (%) for approximately 3 mg of sample extracted from the entrance (sample E_1), middle (sample M_2) and overflow (sample O_3) sections, in five sediment particle size fractions (< 36, [36-63], [63-160], [160-200] and [200-500] µm).

3.3 Occurrence of metals

The metals targeted in our study are known to be contributors to roadway runoff pollution; they stem from vehicular and road wear sources such as engines, tires, brakes, asphalt and road markings (Adachi and Tainosho 2004; Adamiec *et al.* 2016; Allen *et al.* 2017; Grigoratos and Martini 2015; Järlskog *et al.* 2021; Kwak *et al.* 2013; Thorpe and Harrison 2008; Turner and Filella 2023; Zannoni *et al.* 2016). In considering the common sources, their distribution patterns are anticipated to be analogous to those of TRWP.

399 The results of the quantification of the selected metals in the sediment matrix lie within the 10^{2}
400 to 10^{-1} mg/kg of dry sample range (Table 1). The highest concentrations across all samples were
401 found for Zn with a median of 779 ± 8 mg/kg, followed by Cu (178 ± 1 mg/kg), Cr (61.2 ± 0.7
402 mg/kg), V (52.1 ± 0.4 mg/kg), Sb (30.5 ± 0.5 mg/kg), Li (25.1 ± 0.2 mg/kg), Ni (24.6 ± 0.2
403 mg/kg), As (23.4 ± 0.2 mg/kg), Mo (3.46 ± 0.07 mg/kg) and Cd (0.53 ± 0.01 mg/kg). Although
404 these values are broadly comparable to the levels of metals commonly found in similar SuDS
405 (e.g. hundreds of mg/kg for Zn and Cu, and a few tens of mg/kg for Cr and Li) (Allen *et al.*
406 2017; Heal *et al.* 2006; Tedoldi *et al.* 2017), significant discrepancies were nonetheless
407 observed.

408 These variations can be attributed to specific parameters of the stormwater system that govern
409 sediment contamination, such as the nature of the watershed surface (e.g. residential, industrial,
410 road), the water dynamics within the watershed (e.g. precipitation and road washing by
411 municipal services), the number of circulating vehicles, the dimensions and morphology of the
412 infrastructure, as well as the age of the sediment as determined by the frequency of
413 maintenance. Additionally, the technological advancements over time towards reducing the
414 overall emission of metals have also contributed to the discrepancies observed across these
415 studies.

416 The contamination levels of sediments in the infiltration pond were assessed by calculating the
417 EF from a sample extracted at the edge of the pond, to serve as the geochemical background.
418 The EFs indicate a minor enrichment for Cr, Li, Ni and V (EF from 1 to 3), a moderate to major
419 enrichment for Cd (EF 5 to 10), a major enrichment for As, Cu, Mo and Zn (EF 10 to 25), and
420 extreme enrichment for Sb (EF > 50) (further details are given in Table SI-5).

Table 1: Metal concentrations (mg/kg) found in the sediments of the infiltration pond and a geochemical background sample (M_b) extracted from the edge of the pond

Sample	As mg/kg	Cd mg/kg	Cr mg/kg	Cu mg/kg	Li mg/kg	Mo mg/kg	Ni mg/kg	Sb mg/kg	V mg/kg	Zn mg/kg
E_1	19.65 ± 0.67	0.46 ± 0.02	45.12 ± 0.10	127.88 ± 1.04	20.32 ± 0.04	2.68 ± 0.13	19.38 ± 0.28	17.41 ± 0.10	41.78 ± 0.35	630.83 ± 4.73
E_2	17.99 ± 0.09	0.47 ± 0.01	48.12 ± 0.69	109.89 ± 0.17	20.19 ± 0.11	2.37 ± 0.03	20.06 ± 0.82	14.52 ± 1.30	40.17 ± 0.09	550.83 ± 2.68
E_3	19.86 ± 0.74	0.49 ± 0.02	54.65 ± 0.96	140.33 ± 0.82	22.66 ± 0.11	2.53 ± 0.12	22.88 ± 0.18	19.54 ± 0.53	48.68 ± 0.51	720.98 ± 10.99
M_1	18.24 ± 0.31	0.37 ± 0.01	41.80 ± 0.73	114.56 ± 3.33	21.68 ± 0.23	2.31 ± 0.06	19.81 ± 0.47	18.86 ± 0.21	39.22 ± 0.58	528.40 ± 8.03
M_2	23.61 ± 0.04	0.55 ± 0.01	61.21 ± 0.48	178.12 ± 0.03	25.11 ± 0.35	3.69 ± 0.04	24.57 ± 0.08	31.24 ± 0.15	52.10 ± 0.09	779.25 ± 3.18
M_3	26.73 ± 0.11	0.64 ± 0.01	68.81 ± 0.51	191.13 ± 1.86	26.39 ± 0.31	3.67 ± 0.04	27.36 ± 0.20	30.98 ± 0.88	58.11 ± 0.60	881.89 ± 10.51
O_1	23.44 ± 0.23	0.53 ± 0.01	62.10 ± 1.18	185.58 ± 0.59	25.19 ± 0.11	3.46 ± 0.07	25.29 ± 0.01	30.49 ± 0.46	52.94 ± 0.13	805.34 ± 3.28
O_2	28.18 ± 0.23	0.68 ± 0.01	69.81 ± 0.97	255.65 ± 4.67	28.18 ± 0.33	4.80 ± 0.31	28.16 ± 0.19	34.44 ± 0.16	59.80 ± 0.36	1042.90 ± 14.77
O_3	26.73 ± 0.23	0.78 ± 0.05	68.73 ± 2.33	224.43 ± 9.19	28.41 ± 0.52	4.08 ± 0.16	27.58 ± 0.92	33.51 ± 1.47	59.20 ± 1.74	1031.77 ± 38.74
Median	23.44 ± 0.23	0.53 ± 0.01	61.21 ± 0.73	178.12 ± 1.04	25.11 ± 0.23	3.46 ± 0.07	24.57 ± 0.20	30.49 ± 0.46	52.10 ± 0.36	779.25 ± 8.03
M_b	2.01 ± 0.11	0.09 ± 0.04	22.86 ± 0.47	12.66 ± 0.29	15.78 ± 0.02	0.30 ± 0.01	13.72 ± 0.12	0.47 ± 0.01	26.43 ± 0.29	66.07 ± 0.01

3.4 SBR + BR to OM and metals correlation

The distribution of OM content, originating from vegetation decay, microorganisms and anthropogenic sources, e.g. petroleum byproducts, in the Cheviré infiltration pond (Badin *et al.* 2009; Durand *et al.* 2005) ranged from 5.22% to 11.34% of the dry sample. Along with metals, this OM content shows an enrichment towards the overflow section, representing an average increase of 57% for OM and 63% for metals, respectively (Fig. 5).

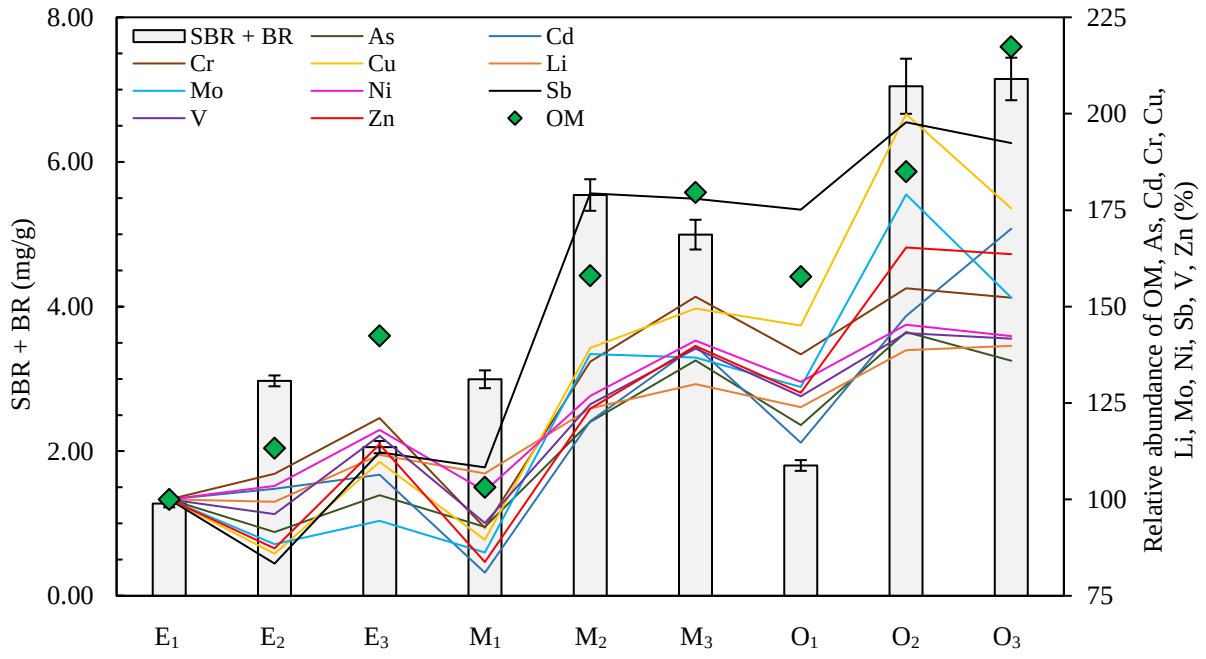

Figure 5: Distribution of SBR + BR (median of replicate, in mg/g, < 500 µm) and the relative abundance of OM (green diamonds), As, Cd, Cr, Cu, Li, Mo, Ni, Sb, V and Zn elements (< 2 mm) (curves) for the entrance (E_1, E_2, E_3), middle (M_1, M_2, M_3) and overflow (O_1, O_2, O_3) sections. For the relative OM and metal abundance, sample E_1 (i.e. the lowest SBR + BR concentration) was set as the reference.

A similar trend had been previously identified in the study by Clozel *et al.* (2006). Notably, the Pearson correlation coefficient between OM and metals ranged from 0.857 to 0.960 ($p < 0.05$) (Table 2), which reinforces the significance of OM as a crucial carrier phase for metals in the sediment matrix. The distinctive features of OM, including its large specific area, abundant sorption sites involving hydroxyl and carboxyl functional groups, and affinity for metals through chemisorption and physisorption, further contribute to the adsorption process and thus

limit both the mobility of ionic elements and bioavailability of metallic compounds in the soil or sediment matrix (He *et al.* 2019; Shi *et al.* 2018; Tedoldi *et al.* 2021). As a result, OM may function as a metal reservoir in such matrices (Sebastia *et al.* 2008).

Moreover, TRWP could potentially function as a carrier phase for metals, as evidenced by the significant positive correlation with SBR + BR. The Shapiro-Wilk test has confirmed the assumption of a high probability of a normal distribution for each variable, with p-values > 0.05 (Table SI 6). All Pearson and Spearman rank coefficients for a confidence level of 95% fell below the 0.05 significance level, with values ranging from 0.739 to 0.824 and 0.720 to 0.945, respectively, for As, Cd, Cr, Cu, Li, Mo, Ni, Sb, V and Zn (Table 2, further details regarding Spearman's rank correlation coefficients and Quantile-Quantile plots for the qualitative assessment are provided in Table SI 7 and Figure SI 4). Rødland *et al.* (2023) first sought to correlate tire wear particles (as quantified by pyrolysis-GC-MS) with Zn, Ni, Pb, Cr, Cu and As metals using soil matrices from nearby roads.

Though surprising, these results showed no significant correlation between tire wear particles and the targeted metals, in a finding similar to that of Unice *et al.*'s (2013) correlations between TRWP from river sediment and brake wear-related metals (i.e. Cu, Pb and Zn). The authors attributed this lack of correlation to the presence of multiple metal sources, different particle transport mechanisms and a higher background level of metals in the matrix. The significant positive correlation identified in our study between SBR + BR and metals, specifically exogeneous metals not originating from the tire tread composition (such as As, V, Cr, Ni, Cu or Sb (Adachi and Tainosho 2004)), confirms the role of TRWP as a pathway for metal contamination in an infiltration pond sediment and/or exhibits analogous behavior, in taking the sedimentary process into account. This correlation points to two likely scenarios of TRWP and metals aggregation processes: one occurring at the tire-road interface, the other within the infiltration pond sediment.

The former process may take place during the formation of TRWP heteroaggregates, wherein abrasion mechanisms incorporate mineral fragments from the road and surface deposits of particulate metals originating from road wear or vehicle-related components (Zannoni *et al.* 2016). As a result, TRWP becomes enriched in metals (Kreider *et al.* 2010), thus contributing to the dissemination of metal contamination into the infiltration pond through runoff. The latter aggregative process is expected to occur within the sediment of the infiltration pond, involving OM that facilitates the relationship between TRWP and particulate and/or dissolved metals. OM is known to be a key agent of aggregation, forming linkages between particles and thereby creating stable heteroaggregates (Badin *et al.* 2009). This effect is suggested by the significant correlation both between OM and metals (median Pearson correlation coefficient $r = 0.950$, p-value < 0.05) and between SBR + BR and OM ($r = 0.801$, p-value < 0.05).

Kovochich *et al.* (2021) reported that as TRWP undergoes aging in a sediment matrix, it forms aggregates not only with minerals but also with other environmental particle sources. Therefore, our data specify that metals and OM could contribute to these aging and aggregation processes in the presence of TRWP. SEM-EDX observations of TRWP particles collected during emissions from our previous study using an instrumented vehicle (De Oliveira *et al.* 2024), as well as the infiltration pond sediment from O_3 sample (i.e. the most contaminated in TRWP), support the aggregative processes of carbonaceous, ocean-derived or terrigenous minerals and metals phases (Figures SI 5 and 6). Moreover, Unice *et al.* (2013) found significant correlations between TRWP and both total organic carbon and finer grain sizes; such findings suggest that TRWP might also be acting as a surrogate for finer materials. From an environmental standpoint and depending on their formation, these heteroaggregates may function as carriers for both metals and tire additives, thereby facilitating the diffusion of a mix of hazardous compounds throughout diverse environmental compartments, including water bodies, soils, sediments and the atmosphere (Järlskog *et al.* 2022).

Table 2: Pearson correlation coefficient (above the gray diagonal) with its associated p-values (below the diagonal).
All p-values lie below the 0.05 significance threshold for SBR + BR, OM and the metals variables

	SBR + BR	OM	As	Cd	Cr	Cu	Li	Mo	Ni	Sb	V	Zn
SBR + BR		0.801	0.795	0.824	0.741	0.792	0.824	0.818	0.762	0.755	0.739	0.778
OM	9.43E-03		0.914	0.954	0.953	0.902	0.960	0.857	0.959	0.894	0.958	0.950
As	1.04E-02	5.63E-04		0.903	0.957	0.968	0.961	0.963	0.966	0.950	0.970	0.963
Cd	6.35E-03	6.75E-05	8.50E-04		0.906	0.885	0.893	0.860	0.892	0.815	0.907	0.943
Cr	2.24E-02	6.99E-05	5.22E-05	7.69E-04		0.927	0.945	0.905	0.989	0.924	0.988	0.947
Cu	1.09E-02	8.73E-04	1.79E-05	1.54E-03	3.28E-04		0.962	0.984	0.946	0.938	0.948	0.978
Li	6.26E-03	4.17E-05	3.66E-05	1.18E-03	1.24E-04	3.36E-05		0.931	0.976	0.966	0.965	0.959
Mo	6.99E-03	3.19E-03	2.98E-05	2.92E-03	8.01E-04	1.55E-06	2.60E-04		0.913	0.937	0.915	0.943
Ni	1.70E-02	4.38E-05	2.26E-05	1.23E-03	4.79E-07	1.17E-04	7.34E-06	5.96E-04		0.943	0.992	0.956
Sb	1.86E-02	1.13E-03	9.05E-05	7.41E-03	3.73E-04	1.82E-04	2.30E-05	1.99E-04	1.37E-04		0.937	0.907
V	2.29E-02	4.69E-05	1.44E-05	7.24E-04	5.37E-07	1.02E-04	2.64E-05	5.43E-04	1.80E-07	1.97E-04		0.972
Zn	1.36E-02	8.62E-05	3.07E-05	1.36E-04	1.07E-04	5.43E-06	4.41E-05	1.39E-04	5.51E-05	7.26E-04	1.13E-05	

3.5 Infiltration pond as a sink for TRWP

We next evaluated the pond's theoretical effectiveness in retaining TRWP by estimating both the inflow of TRWP into the pond and the total amount retained in the sediment by means of Equations 2 and 3, respectively. TRWP inflow was grounded in realistic TRWP emissions, specifically using the TRWP emission value derived from the tire weight loss (TWL) parameter. Our previous study on realistic emissions, conducted with an instrumented vehicle, determined the TWL for the right front driving wheel equal to 11.0 mg of tire per km, or 16.6 mg of TRWP per km for the ring road track connecting to the Cheviré infiltration pond (De Oliveira *et al.* 2024). In assuming a TRWP emissions per vehicle per km with a wheel contribution factor (W) of 2.7 (Luhana *et al.* 2004), a traffic density (T) of 88,500 vehicles per day, a time frame (t) of 247 days and a given distance (d) from the southern section of the bridge (i.e. 0.8 km), the theoretical inflow of TRWP into the pond could be approximated at 780 kg (Fig. 6). We then compared this value with the accumulated and retained TRWP in the sediment.

To estimate the amount of TRWP retained in the sediment, we considered three sediment density hypotheses (ρ_1, ρ_2, ρ_3), corresponding to silt, TRWP and coarser sediments (with densities of 1.3, 1.8 and 2.6 g/cm^3), respectively. The amounts estimated from ρ_1 and ρ_3 were deliberately based on extreme density scenarios: either the sediment consists entirely of silt or entirely of coarse sediment. This approach allowed us to establish rough constraints for low and high estimates. For ρ_2 however, the density selected was closer to the actual nature of the sediments studied. All three calculations were based on: the surface area of each section, a gradual sediment thickness of 1 cm, 1.5 cm and 2 cm from entrance to overflow, a median SBR + BR concentration per section, and a mean SBR + BR-to-TRWP conversion factor of 9.12, as obtained from the literature (Klöckner *et al.* 2021; Kreider *et al.* 2010; Rauert *et al.* 2021; Sommer *et al.* 2018; Unice *et al.* 2012).

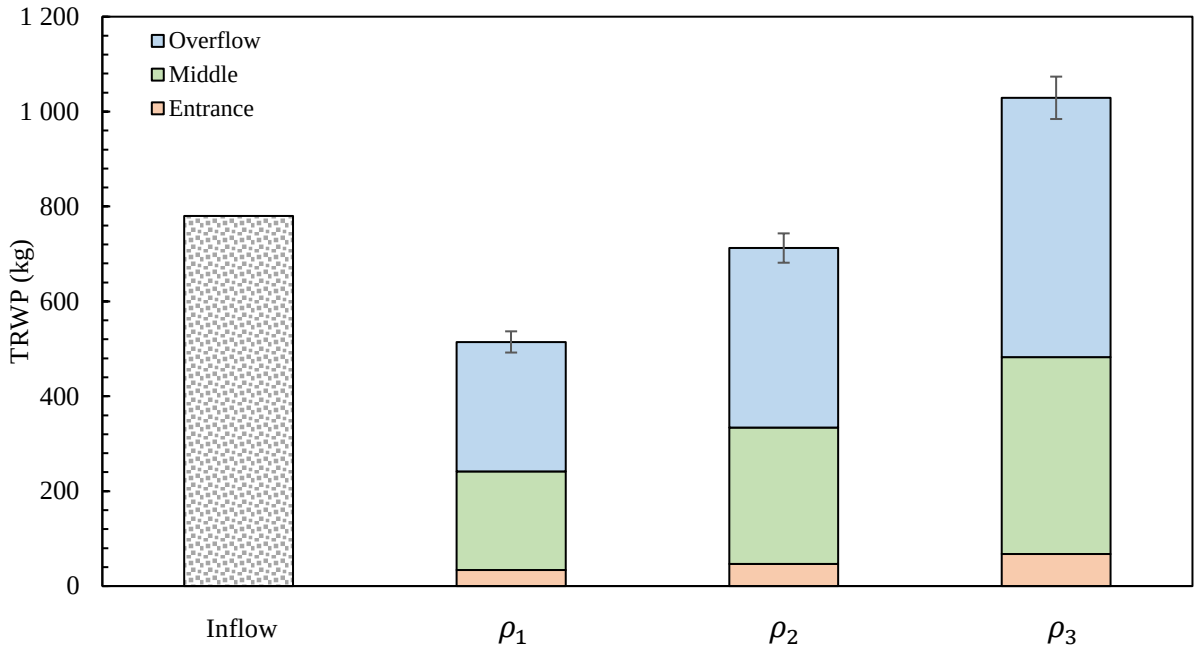

Figure 6: Estimation of the TRWP content (kg) retained within the sediment based on three hypotheses (ρ_1, ρ_2, ρ_3), as outlined in Section 3.5, along with an estimation of the TRWP amount (kg) as inflow to the infiltration pond derived from realistic emissions, as reported in our previous study (De Oliveira *et al.* 2024) (gray dotted histogram bar). The error bars for ρ_1, ρ_2 and ρ_3 represent the standard deviation of the triplicates obtained from the results discussed in Section 3.1. The error bar for inflow has been derived from the TWL result, whose measurement variation equals 0.1% and is therefore indistinguishable from the line thickness of the histogram.

The results obtained were: 515 ± 22, 712 ± 31 and 1,029 ± 45 kg of TRWP for ρ_1, ρ_2 and ρ_3, respectively. Since, ρ_2 better reflects the characteristics of the sediment, it is noteworthy that the amount of TRWP retained in the infiltration pond is comparable to the inflow. Despite the assumptions adopted during the calculations and the potential for vertical TRWP migration into the substratum or a small fraction of tire wear not reaching the infiltration pond, both values remain lie on the same order of magnitude, i.e. approximately 700 to 800 kg of TRWP.

These findings indicate that only a small fraction of TRWP is transferred to the atmosphere, with the majority remaining and evolving at the road surface (as confirmed by our previous study, see De Oliveira *et al.* (2024)). In addition, a large fraction of TRWP is remobilized from road surfaces by runoff, ultimately heading towards the infiltration pond. Moreover, the mass balance supports limited vertical TRWP enrichment of the substratum, thus confirming that the Cheviré infiltration pond function is an efficient infrastructure for retaining TRWP and preventing their dispersal into the downstream environment. The potential of an infiltration pond to act as a TRWP sink has also been confirmed, to a similar extent as what has been reported for other microplastics by García-Haba *et al.* (2023) and Olesen *et al.* (2019), with sedimentation processes playing a key role in microplastic retention. More specifically, Gilbreath *et al.* (2019) estimated a reduction in microplastic concentrations of between 83% and 95% in a bioretention system. Similarly, Smyth *et al.* (2021) observed reductions exceeding 80% throughout a bioretention cell, while Jakubowicz *et al.* (2022) documented a minimum reduction efficiency of 77% for microplastics in a multistage constructed wetland.

3.6 Uncertainties and future challenges

Several inherent uncertainties arise when studying TRWP environmental contamination, particularly when relying on mass spectrometry methods. Among these uncertainties, three critical points are highly relevant to the scientific community and will be discussed below.

The first point pertains to the specificity of the pyrolytic markers. As highlighted by Rødland *et al.* (2022), the accuracy of rubber quantification is heavily dependent on the markers used to identify and quantify TRWP heteroaggregates. To address the uncertainty associated with the variations in single markers, these authors employed a method based on a combination of four different pyrolysis products, namely benzene, α-methylstyrene, ethylstyrene and a butadiene trimer to assess SBR + BR content in tires, as well as the styrene-butadiene-styrene (SBS)

content in polymer-modified bitumen used in some road asphalt. Our study has adopted a similar approach, in targeting two specific markers to evaluate SBR + BR content. However, as noted by Rødland *et al.* (2022), SBR and SBS polymers share similar pyrolytic markers, such as the 4-VCH, with some SBS markers overlapping those of BR. To assess the potential overestimation of TRWP concentration, the authors recommend initially investigating the presence of SBS in the road surface prior to analyzing samples for SBR or BR. In the context of our study, conducting this preliminary analysis is currently infeasible due to restricted access to the bridge road, thus preventing *in situ* sampling. One potential solution would be to obtain detailed information on the bitumen composition from industries, which could then be uploaded to a collaborative open-source database, as proposed by Rødland and Lin (2023) for tire composition. Alternatively, employing a more selective analytical technique, such as tandem or high-resolution mass spectrometry, could facilitate the targeted analysis of SBR or BR while minimizing interference from SBS. Another solution would be to perform a quantification based on just 4-PCH as a marker for SBR, which would then eliminate interference from SBS since this marker is not produced by the SBS polymer.

The second point is the aging of TRWP. Given that these particles age in the environment, they undergo various physical and chemical transformations capable of affecting both the polymeric content of TRWP and their pyrolytic markers, hence potentially impacting the accuracy of quantification (Rødland *et al.* 2022; Wagner *et al.* 2022). This consideration calls into question a key assumption in many studies, including ours, regarding the assessment of TRWP in the environment, namely: the pyrolysis of environmental TRWP, despite their aging and the potential oxidation of their polymeric fractions over time, has a pyrolytic yield equivalent to that of tire tread or SBR and BR standards, which have not undergone any chemical or physical transformations.

In addition of aging process, the impact of vulcanization on the pyrolytic yield of the polymeric fraction in tires, compared to unvulcanized polymer standards, is also an important area of research worth considering. Vulcanization is known to influence rubber cracking and promote key processes such as dehydrogenation, aromatization and polymerization during pyrolysis (Sun *et al.* 2022). Further investigation is thus required to fully understand how exactly environmental aging and vulcanization influences the reliability of Pyr-GC-MS analyses in quantifying TRWP.

The third and final point concerns the representativeness of the SBR + BR-to-TRWP conversion factor. The main limitation herein lies in the consistency between the polymeric content of the samples and that of the tires, as well as the encrusted particle content of TRWP (Klöckner *et al.* 2021; Rødland *et al.* 2022). Variations in tire brand, tire type (winter, summer, all-season), vehicle weight and type (thermal or electric), market location, sampling site, road conditions, type of bitumen, and traffic density can all influence both the polymeric and mineral content of TRWP. These factors inevitably introduce a level of approximation when calculating the equivalent amount of SBR + BR in TRWP. To minimize this level of approximation, we have calculated the TRWP content using a median SBR + BR-to-TRWP conversion factor of 9.12, which accounts for both the minimum and maximum levels of particle encrustment and polymeric content (Kreider *et al.* 2010; Rauert *et al.* 2021; Sommer *et al.* 2018; Unice *et al.* 2012). This approach could be further refined with access to a representative mix of tire brands and types used in France or Europe, in providing a more accurate estimate of the average polymeric content. However, without a specific *in situ* assessment of TRWP encrustment and/or density, relying on a median value of encrustment from the literature remains the most practical solution. It is obvious that future studies assessing tire particles in the environment should systematically include both the quantified content of the polymeric fractions, based on the selected polymer, and the corresponding conversion factors for estimating TWP or TRWP

608 equivalence. This approach is aimed at progressively standardizing methodologies and ensuring
609 consistency across studies, thereby empowering researchers to accurately compare data and
610 facilitate future meta-analyses, in ultimately leading to a better understanding of the
611 environmental implications of these tire particles.

612 Although these uncertainties are present in our study, we still anticipate that the regular
613 introduction of freshly generated TRWP into the infiltration pond may mitigate the effects of
614 aging on the overall TRWP concentrations over the short 8-month period of sediment
615 accumulation. Moreover, the estimated amount of TRWP inflow, based on the realistic local
616 weight loss of tires, and the TRWP amount retained in the sediment remain relatively close, i.e.
617 with a difference of < 9%. This finding supports the notion that the SBS pyrolytic interferences
618 with SBR or BR, as well as the potential effects of aging on polymeric quantification, are likely
619 to be limited. If present, these factors might account for a maximum variation of 9% in our
620 study. As for the reliability of this conversion factor, it does not affect the overall trend observed
621 within the infiltration pond but may call into question the TRWP values when compared to
622 other studies using different conversion factors.

623 To shed new light on the formation of TRWP heteroaggregates and given that our data suggest
624 metals and organic matter contribute to the aggregation process in the presence of TRWP, a
625 more in-depth characterization of the surface properties and reactivity becomes imperative.
626 This step is crucial due to the current lack of such information in the scientific literature and
627 when considering the possible adsorption of dissolved metals. Moreover, increasing the number
628 of sampling points to achieve a better distribution across the pond and comparing SBR + BR
629 with the OM and metals variables within the same size fraction and granulometric range is
630 expected to significantly refine the correlation, improve the statistical representativeness of the
631 data and help determine whether the observed associations between TRWP with OM and metals
632 are causal. These future steps are particularly important given that we currently possess a

limited number of observation (i.e. nine samples), as compared to the number of variables (i.e. twelve variables including SBR + BR, OM and metals), and have used different sieving thresholds of 500 µm for TRWP and 2 mm for OM and metals analysis (see Sections 2.3 and 2.4). Additionally, further analysis using SEM and EDX techniques would be necessary to characterize the intricate relationship of heteroaggregates containing OM, metals and TRWP within the sediment. From these findings, utilization of the SBR + BR polymeric fraction from tires could serve as a reliable indicator of metal contamination in stormwater systems.

On a broader level and from a management perspective, data are currently lacking on TRWP contamination thresholds in environmental matrices, notably in stormwater systems sediment. Establishing these thresholds is crucial to determining the stormwater system maintenance schedule and the fate of the sediment post-removal as regards TRWP contamination. Collaborative efforts by the scientific community and public policymakers should be directed at bridging this gap.

One innovative approach to addressing this gap entails considering SBR + BR not only as a proxy for TRWP but also as an indicator of metal contamination in the stormwater system environment. Comprehensive analyses across multiple stormwater system sites are essential, in order to examine both SBR + BR levels and metal pollution while accounting for variations in watershed surface use and traffic density. Subsequently, we could propose an innovative and novel correlation factor between SBR + BR and metals, to facilitate the assessment of TRWP or metal levels, whereby one can be used as a proxy for the other depending on the analytical methods available (e.g. Pyr-GC-MS, ICP-MS or portable X-ray fluorescence). In addition, by using such a correlation, preliminary TRWP thresholds could be established for sediment matrices based on existing metal contaminant thresholds, thereby serving to both determine the hazardous sediment level and schedule stormwater system maintenance that targets TRWP by means of Pyr-GC-MS.

3.7 Management recommendations

The implementation of optimized sediment removal practices is invaluable for mitigating the potential of a SuDS to become a source of pollution when cleaning actions are neglected (Humphrey *et al.* 2023). Numerous studies have revealed that SuDS can achieve high retention rates, exceeding 79% and sometimes reaching up to 100%, for total suspended solids as well as for contaminants such as polychlorinated biphenyls, polycyclic aromatic hydrocarbons, total nitrogen, total phosphorus, mainly due to their affinity for fine sediment particles and ability to settle (DeBusk and Wynn, 2011; Gilbreath *et al.* 2019; Jakubowicz *et al.* 2022; Maurer *et al.* 2021). In light of these studies and our findings demonstrating that infiltration ponds are also capable of retaining TRWP, high retention rates would imply a progressive accumulation of contaminants in the sediment layer. Attention therefore must still be drawn to potential stormwater systems limitations as regards hazardous TRWP constituents.

The inherent nature of the Cheviré infiltration pond, as characterized by the absence of an impermeable layer at the bottom, combines with intricate physicochemical and biological processes within the pond, leading over time to the photooxidation and microbial degradation of TRWP heteroaggregates and, hence, the leaching of hazardous constituents (Baensch-Baltruschat *et al.* 2020; Ding *et al.* 2023; Klun *et al.* 2023; Wagner *et al.* 2022). Metals, in particular, can leach into and accumulate in sediments, with some elements being easily remobilized due to their intrinsic mobility and affinity for the dissolved phase. These processes are influenced by physicochemical parameters of the medium, such as pH, ionic strength, competing ions, sorption sites and their affinity for dissolved organic matter. Under specific conditions, it is not uncommon for certain metals, such as copper or nickel, to exhibit poor or even negative retention rates (Humphrey *et al.* 2023; Jakubowicz *et al.* 2022).

This outcome raises concerns over the spread of such environmental micropollutants (Maurer *et al.* 2021). The infiltration of micropollutants, including those from TRWP leachates, deep into the alluvial substratum of the Loire River beneath the pond and, consequently, into groundwater contaminating water bodies (Tedoldi *et al.* 2017) can indeed be anticipated. It therefore becomes necessary to analyze core samples taken from the infiltration pond substratum in order to assess: i) the occurrence and concentration of the targeted micropollutants over substratum depth, and ii) overall relevance of the infiltration pond relative to a broader hazardous spectrum (Maurer *et al.* 2021).

The acquisition of data regarding contamination levels of TRWP and their spatial distribution in a stormwater system is necessary to establish an effective water management strategy. Chemical analysis targeting TRWP, coupled with a topographic and size fractionation assessment, has revealed the pollutant footprint of the entire Cheviré infiltration pond. The information gathered can then serve as a foundation for developing a cost-effective remediation strategy by means of prioritizing specific sections of the infiltration pond, namely the most contaminated ones. The recommended strategy involves cleaning efforts in areas 2 and 3, located in the middle and overflow sections, before addressing sediment removal in the entrance section and area 1. This strategic sequence would aim to efficiently target and address the areas of maximum TRWP accumulation. Given the intricate relationship between TRWP and metals, such a cleaning effort intended for TRWP removal will also effectively remove metals by focusing on the same areas of accumulation, thereby optimizing the overall remediation process.

Although infiltration ponds offer the advantage of capturing and retaining a significant amount of TRWP, as well as a fraction of the associated metal pollutants, their implementation in areas with high anthropogenic pressure and high traffic density, e.g. urban centers, remains highly challenging. Several major constraints are to be considered. First, the number, size and

associated costs of these installations will depend on the drained surface area and expected volume of particulate runoff, yet densely populated areas offer limited to no space for constructing such infrastructure. Second, infiltrated water could potentially damage nearby preexisting infrastructure, such as underground electrical networks. Third, soil quality in urban areas is often compacted, thus making it unsuitable for effective infiltration. Fourth and last is the presence of a groundwater table contamination risk (U.S. EPA, 2021). Under these conditions, infiltration ponds are preferentially constructed in suburban areas. One potential solution could be to adapt existing urban drainage infrastructure by increasing the use of gully pots with sediment traps. This approach has proven to effectively trap a variety of organic and particulate contaminants, such as microplastics and TRWP (Mengistu *et al.* 2021; Öborn *et al.* 2024; Rødland *et al.* 2023; Wei *et al.* 2023). However, gully pots cover a much smaller drainage area and have limited capacity, as compared to infiltration ponds. Therefore, it would seem crucial to increase the number of gully pots and ensure their regular maintenance, including frequent cleaning of the sediment trap. Like with infiltration ponds, without proper maintenance, gully pots are at risk of sediment remobilization during heavy rainfall events and/or lixiviation of TRWP, which could further propagate pollution through the pipe network and, ultimately, into water bodies if discharges are directly connected.

4. Conclusion

This study has significantly contributed to enhancing knowledge on the fate of TRWP within an infiltration pond and moreover emphasizes the pivotal role of such infrastructure in managing TRWP pollution. Through a sampling strategy covering the surface of the Cheviré infiltration pond and leveraging a multi-characterization technique, namely the pyrolysis-GC-MS method, to target the polymeric signature of tires, we have been able to address the points raised in the introduction and have derived the following key findings:

i. Extensive SBR + BR contamination of the infiltration pond sediment has been found to lie in the mg/g range, but at various degrees depending on the location of the sample, with enrichment towards the overflow. Two sections (i.e. middle and overflow) have been identified as major zones of SBR + BR accumulation, which aligns with the topographic configuration of the pond.

ii. The size fractionation of SBR + BR within the sediment reveals a bimodal distribution, thus indicating two distinct types of TRWP. The one characterized by a smaller size (63-160 µm) suggests TRWP less aged and aggregated with other environmental particles. The second type, characterized by a larger particle size (200-500 µm), suggests higher environmental particle encrustation and thus more aged TRWP.

iii. A strong correlation has been detected between SBR + BR and metals, such as As, Cd, Cr, Cu, Li, Mo, Ni, Sb, V and Zn. This relationship can be attributed to either the preexistence of metals in the tire composition or the incorporation of metals not originating from the tire. This type of incorporation occurs during the formation of TRWP heteroaggregates at the road surface and/or within the sediment, with organic matter facilitating the process.

iv. The approximate mass balance estimation between TRWP inflow from realistic tire loss and the amount retained within the sediment supports a limited mass transfer of TRWP emissions to the atmosphere and has moreover confirmed the role of an infiltration pond as a major sink for TRWP from runoff.

This study paves the way for an effective management strategy of stormwater system sediments contaminated with TRWP. Given the wide range of contaminants in stormwater system sediment, including metals, we would recommend focusing cleaning efforts on those areas with the highest TRWP accumulation. In conclusion, let's reiterate the importance of conducting routine chemical analyses on sediment from stormwater systems. This practice is indeed essential to enhancing management strategies aimed at ensuring that such infrastructure, and more specifically infiltration ponds intended as sinks, does not evolve into sources of pollution for the downstream environment.

Funding sources

As part of the Plasti-nium Research Project, this work has been funded by France's Loire Valley Region and the Nantes Metropolitan Council. This study was also supported by the Region Pays-de-la Loire which financed the PhD grant of DPT Dang along with Gustave Eiffel University. The Cheviré pond is one of the sites monitored in the Nantes Urban Environment Observatory (ONEVU-IRSTV) and the National Observation Service Observil (SNO Observil). IRSTV (CNRS-FR2488) and OSUNA financially supported the data collection.

Declaration of interests

The authors hereby declare that they have no known competing financial interests or personal relationships that could have appeared to influence the work reported in this paper.

Acknowledgements

This work has received support as part of the program "Investissement d'Avenir" launched by the French Government and implemented by the National Research Agency (ANR), under the reference ANR-16-IDEX-0003. The authors would also like to express their gratitude to Dr. Yang, the three anonymous reviewers for their constructive comments and Mathieu Goriaux for his valuable contribution in performing the SEM-EDX analysis.

References

Adachi, K., Tainosho, Y., 2004. Characterization of heavy metal particles embedded in tire dust. Environ. Int. 30, 1009–1017. https://doi.org/10.1016/j.envint.2004.04.004

Adamiec, E., Jarosz-Krzemińska, E., Wieszała, R., 2016. Heavy metals from non-exhaust vehicle emissions in urban and motorway road dusts. Environ. Monit. Assess. 188, 369. https://doi.org/10.1007/s10661-016-5377-1

Allen, D., Haynes, H., Arthur, S., 2017. Contamination of Detained Sediment in Sustainable Urban Drainage Systems. Water 9, 355. https://doi.org/10.3390/w9050355

Badin, A.-L., Méderel, G., Béchet, B., Borschneck, D., Delolme, C., 2009. Study of the aggregation of the surface layer of Technosols from stormwater infiltration basins using grain size analyses with laser diffractometry. Geoderma 153, 163–171. https://doi.org/10.1016/j.geoderma.2009.07.022

Baensch-Baltruschat, B., Kocher, B., Stock, F., Reifferscheid, G., 2020. Tyre and road wear particles (TRWP) - A review of generation, properties, emissions, human health risk, ecotoxicity, and fate in the environment. Sci. Total Environ. 733, 137823. https://doi.org/10.1016/j.scitotenv.2020.137823

Capolupo, M., Sørensen, L., Jayasena, K.D.R., Booth, A.M., Fabbri, E., 2020. Chemical composition and ecotoxicity of plastic and car tire rubber leachates to aquatic organisms. Water Res. 169, 115270. https://doi.org/10.1016/j.watres.2019.115270

Clozel, B., Ruban, V., Durand, C., Conil, P., 2006. Origin and mobility of heavy metals in contaminated sediments from retention and infiltration ponds. Appl. Geochem. 21, 1781–1798. https://doi.org/10.1016/j.apgeochem.2006.06.017

Dang, D.P.T., Jean-Soro, L., Béchet, B., 2023. Pollutant characteristics and size distribution of trace elements during stormwater runoff events. Environ. Chall. 11, 100682. https://doi.org/10.1016/j.envc.2023.100682

DeBusk, K.M., Wynn, T.M., 2011. Storm-Water Bioretention for Runoff Quality and Quantity Mitigation. Journal of Environmental Engineering 137, 800–808. https://doi.org/10.1061/(ASCE)EE.1943-7870.0000388

De Oliveira, T., Muresan, B., Ricordel, S., Lumière, L., Truong, X.-T., Poirier, L., Gasperi, J., 2024. Realistic assessment of tire and road wear particle emissions and their influencing factors on different types of roads. J. Hazard. Mater. 465, 133301. https://doi.org/10.1016/j.jhazmat.2023.133301

Ding, J., Lv, M., Zhu, D., Leifheit, E.F., Chen, Q.-L., Wang, Y.-Q., Chen, L.-X., Rillig, M.C., Zhu, Y.-G., 2023. Tire wear particles: An emerging threat to soil health. Crit. Rev. Environ. Sci. Technol. 53, 239–257. https://doi.org/10.1080/10643389.2022.2047581

Dudefoi, W., Ferrari, B.J.D., Breider, F., Masset, T., Leger, G., Vermeirssen, E., Bergmann, A.J., Schirmer, K., 2024. Evaluation of tire tread particle toxicity to fish using rainbow trout cell lines. Sci. Total Environ. 912, 168933. https://doi.org/10.1016/j.scitotenv.2023.168933

Durand, C., Ruban, V., Amblès, A., 2005. Characterisation of complex organic matter present in contaminated sediments from water retention ponds. J. Anal. Appl. Pyrolysis 73, 17–28. https://doi.org/10.1016/j.jaap.2004.09.001

Eisentraut, P., Dümichen, E., Ruhl, A.S., Jekel, M., Albrecht, M., Gehde, M., Braun, U., 2018. Two Birds with One Stone—Fast and Simultaneous Analysis of Microplastics: Microparticles Derived from Thermoplastics and Tire Wear. Environ. Sci. Technol. Lett. 5, 608–613. https://doi.org/10.1021/acs.estlett.8b00446

El-Mufleh, A., Béchet, B., Ruban, V., Legret, M., Clozel, B., Barraud, S., Gonzalez-Merchan, C., Bedell, J.-P., Delolme, C., 2014. Review on physical and chemical characterizations of contaminated sediments from urban stormwater infiltration basins within the framework of the French observatory for urban hydrology (SOERE URBIS). Environ. Sci. Pollut. Res. Int. 21, 5329–5346. https://doi.org/10.1007/s11356-013-2490-3

EN 15935, Soil, waste, treated biowaste and sludge - Determination of loss on ignition, 2021.

Färm, C., 2002. Evaluation of the accumulation of sediment and heavy metals in a storm-water detention pond. Water Sci. Technol. 45, 105–112. https://doi.org/10.2166/wst.2002.0122

Federico, L., Masseroni, A., Rizzi, C., Villa, S., 2023. Silent Contamination: The State of the Art, Knowledge Gaps, and a Preliminary Risk Assessment of Tire Particles in Urban Parks. Toxics 11, 445. https://doi.org/10.3390/toxics11050445

Gaggini, E.L., Polukarova, M., Bondelind, M., Rødland, E., Strömvall, A.-M., Andersson-Sköld, Y., Sokolova, E., 2024. Assessment of fine and coarse tyre wear particles along a highway stormwater system and in receiving waters: Occurrence and transport. Journal of Environmental Management 367, 121989. https://doi.org/10.1016/j.jenvman.2024.121989

García-Haba, E., Hernández-Crespo, C., Martín, M., Andrés-Doménech, I., 2023. The role of different sustainable urban drainage systems in removing microplastics from urban runoff: A review. J. Clean. Prod. 411, 137197. https://doi.org/10.1016/j.jclepro.2023.137197

German, J., Svensson, G., 2005. Stormwater pond sediments and water—characterization and assessment. Urban Water J. 2, 39–50. https://doi.org/10.1080/15730620500042536

Gilbreath, A., McKee, L., Shimabuku, I., Lin, D., Werbowski, L.M., Zhu, X., Grbic, J., Rochman, C., 2019. Multiyear Water Quality Performance and Mass Accumulation of PCBs, Mercury, Methylmercury, Copper, and Microplastics in a Bioretention Rain Garden. Journal of Sustainable Water in the Built Environment 5, 04019004. https://doi.org/10.1061/JSWBAY.0000883

Goßmann, I., Halbach, M., Scholz-Böttcher, B.M., 2021. Car and truck tire wear particles in complex environmental samples – A quantitative comparison with "traditional" microplastic polymer mass loads. Sci. Total Environ. 773, 145667. https://doi.org/10.1016/j.scitotenv.2021.145667

Grigoratos, T., Martini, G., 2015. Brake wear particle emissions: a review. Environ. Sci. Pollut. Res. Int. 22, 2491–2504. https://doi.org/10.1007/s11356-014-3696-8

He, Y., Men, B., Yang, X., Li, Y., Xu, H., Wang, D., 2019. Relationship between heavy metals and dissolved organic matter released from sediment by bioturbation/bioirrigation. J. Environ. Sci. 75, 216–223. https://doi.org/10.1016/j.jes.2018.03.031

Heal, K.V., Hepburn, D.A., Lunn, R.J., 2006. Sediment management in sustainable urban drainage system ponds. Water Sci. Technol. J. Int. Assoc. Water Pollut. Res. 53, 219–227. https://doi.org/10.2166/wst.2006.315

Humphrey, J., Rowett, C., Tyers, J., Gregson, M., Comber, S., 2023. Are sustainable drainage systems (SuDS) effective at retaining dissolved trace elements? Environ. Technol. 44, 1450–1463. https://doi.org/10.1080/09593330.2021.2004454

ISO 7270-1, Rubber - Analysis by pyrolytic gas-chromatography methods - Part 1: Identification of polymers (single polymers and polymer blends), 2017.

ISO 11464, Soil quality - Pretreatment of samples for physico-chemical analysis, 2006.

ISO 11885, Water quality - Determination of selected elements by inductively coupled plasma optical emission spectrometry (ICP-OES), 2007.

ISO 14869-1, Soil quality - Dissolution for the determination of total element content - Part 1: Dissolution with hydrofluoric and perchloric acids, 2001.

Jakubowicz, P., Fitobór, K., Gajewska, M., Drewnowska, M., 2022. Detection and Removal of Priority Substances and Emerging Pollutants from Stormwater: Case Study of the Kołobrzeska Collector, Gdańsk, Poland. Sustainability 14, 1105. https://doi.org/10.3390/su14031105

Järlskog, I., Jaramillo-Vogel, D., Rausch, J., Gustafsson, M., Strömvall, A.-M., Andersson-Sköld, Y., 2022. Concentrations of tire wear microplastics and other traffic-derived non-exhaust particles in the road environment. Environ. Int. 170, 107618. https://doi.org/10.1016/j.envint.2022.107618

Järlskog, I., Strömvall, A.-M., Magnusson, K., Galfi, H., Björklund, K., Polukarova, M., Garção, R., Markiewicz, A., Aronsson, M., Gustafsson, M., Norin, M., Blom, L., Andersson-Sköld, Y., 2021. Traffic-related microplastic particles, metals, and organic pollutants in an urban area under reconstruction. Sci. Total Environ. 774, 145503. https://doi.org/10.1016/j.scitotenv.2021.145503

Jiang, J.-R., Chen, Z.-F., Liao, X.-L., Liu, Q.-Y., Zhou, J.-M., Ou, S.-P., Cai, Z., 2023. Identifying potential toxic organic substances in leachates from tire wear particles and their mechanisms of toxicity to Scenedesmus obliquus. J. Hazard. Mater. 458, 132022. https://doi.org/10.1016/j.jhazmat.2023.132022

Klöckner, P., Reemtsma, T., Eisentraut, P., Braun, U., Ruhl, A.S., Wagner, S., 2019. Tire and road wear particles in road environment - Quantification and assessment of particle dynamics by Zn determination after density separation. Chemosphere 222, 714–721. https://doi.org/10.1016/j.chemosphere.2019.01.176

Klöckner, P., Seiwert, B., Weyrauch, S., Escher, B.I., Reemtsma, T., Wagner, S., 2021. Comprehensive characterization of tire and road wear particles in highway tunnel road dust by use of size and density fractionation. Chemosphere 279, 130530. https://doi.org/10.1016/j.chemosphere.2021.130530

Klun, B., Rozman, U., Kalčíková, G., 2023. Environmental aging and biodegradation of tire wear microplastics in the aquatic environment. J. Environ. Chem. Eng. 11, 110604. https://doi.org/10.1016/j.jece.2023.110604

Kole, P.J., Löhr, A.J., Van Belleghem, F.G.A.J., Ragas, A.M.J., 2017. Wear and Tear of Tyres: A Stealthy Source of Microplastics in the Environment. Int. J. Environ. Res. Public. Health 14, 1265. https://doi.org/10.3390/ijerph14101265

Koutnik, V.S., Leonard, J., Glasman, J.B., Brar, J., Koydemir, H.C., Novoselov, A., Bertel, R., Tseng, D., Ozcan, A., Ravi, S., Mohanty, S.K., 2022. Microplastics retained in stormwater control measures: Where do they come from and where do they go? Water Res. 210, 118008. https://doi.org/10.1016/j.watres.2021.118008

Kovochich, M., Parker, J.A., Oh, S.C., Lee, J.P., Wagner, S., Reemtsma, T., Unice, K.M., 2021. Characterization of Individual Tire and Road Wear Particles in Environmental Road Dust, Tunnel Dust, and Sediment. Environ. Sci. Technol. Lett. 8, 1057–1064. https://doi.org/10.1021/acs.estlett.1c00811

Kreider, M.L., Panko, J.M., McAtee, B.L., Sweet, L.I., Finley, B.L., 2010. Physical and chemical characterization of tire-related particles: Comparison of particles generated using different methodologies. Sci. Total Environ. 408, 652–659. https://doi.org/10.1016/j.scitotenv.2009.10.016

Kwak, J., Kim, H., Lee, J., Lee, S., 2013. Characterization of non-exhaust coarse and fine particles from on-road driving and laboratory measurements. Sci. Total Environ. 458–460, 273–282. https://doi.org/10.1016/j.scitotenv.2013.04.040

Ledieu, L., Tramoy, R., Ricordel, S., Astrie, D., Tassin, B., Gasperi, J., 2022. Amount, composition and sources of macrolitter from a highly frequented roadway. Environ. Pollut. 303, 119145. https://doi.org/10.1016/j.envpol.2022.119145

Li, K., Hao, W., Liu, C., Chen, Z., Ye, Z., 2024. Ecotoxicity of tire wear particles to antioxidant enzyme system and metabolic functional activity of river biofilms: The strengthening role after incubation-aging in migrating water phases. Sci. Total Environ. 914, 169849. https://doi.org/10.1016/j.scitotenv.2023.169849

Luhana, L., Sokhi, R., Warner, L., Mao, H., Boulter, P., McCrae, I., Wright, J., Reeves, N., Osborn, D., 2004. Non-exhaust particulate measurements: results. Deliverable 8 of the European Commission DG TREN 5th Framework Particulates project. https://www.google.com/url?sa=t&rct=j&q=&esrc=s&source=web&cd=&ved=2ahUKEwjg1MblgdOCAxWGVqQEHfXsAcAQFnoECA4QAQ&url=https%3A%2F%2Fwww.groundsmartrubbermulch.com%2Fdocs%2Fresources%2FMeasurement-of-non-exhaust-particulate-matter.pdf&usg=AOvVaw2rZAqblu-8M1NmH3Tbq5Ar&opi=89978449

Maurer, L., Zumsteg, J., Lutz, C., Ottermatte, M.P., Wanko, A., Heintz, D., Villette, C., 2021. Towards a model for road runoff infiltration management. Npj Clean Water 4, 1–9. https://doi.org/10.1038/s41545-021-00136-z

Mengistu, D., Heistad, A., Coutris, C., 2021. Tire wear particles concentrations in gully pot sediments. Sci. Total Environ. 769, 144785. https://doi.org/10.1016/j.scitotenv.2020.144785

Müller, K., Hübner, D., Huppertsberg, S., Knepper, T.P., Zahn, D., 2022. Probing the chemical complexity of tires: Identification of potential tire-borne water contaminants with high-resolution mass spectrometry. Sci. Total Environ. 802, 149799. https://doi.org/10.1016/j.scitotenv.2021.149799

Öborn, L., Österlund, H., Viklander, M., 2024. Microplastics in gully pot sediment in urban areas: Presence, quantities and characteristics. Environmental Pollution 353, 124155. https://doi.org/10.1016/j.envpol.2024.124155

Olesen, K.B., Stephansen, D.A., van Alst, N., Vollertsen, J., 2019. Microplastics in a Stormwater Pond. Water 11, 1466. https://doi.org/10.3390/w11071466

Österlund, H., Blecken, G., Lange, K., Marsalek, J., Gopinath, K., Viklander, M., 2023. Microplastics in urban catchments: Review of sources, pathways, and entry into stormwater. Sci. Total Environ. 858, 159781. https://doi.org/10.1016/j.scitotenv.2022.159781

Page, T.S., Almeda, R., Koski, M., Bournaka, E., Nielsen, T.G., 2022. Toxicity of tyre wear particle leachates to marine phytoplankton. Aquat. Toxicol. 252, 106299. https://doi.org/10.1016/j.aquatox.2022.106299

Peng, W., Liu, C., Chen, D., Duan, X., Zhong, L., 2022. Exposure to N-(1,3-dimethylbutyl)-N′-phenyl-p-phenylenediamine (6PPD) affects the growth and development of zebrafish embryos/larvae. Ecotoxicol. Environ. Saf. 232, 113221. https://doi.org/10.1016/j.ecoenv.2022.113221

952 Rauert, C., Rødland, E.S., Okoffo, E.D., Reid, M.J., Meland, S., Thomas, K.V., 2021.
953 Challenges with Quantifying Tire Road Wear Particles: Recognizing the Need for Further
954 Refinement of the ISO Technical Specification. Environ. Sci. Technol. Lett. 8, 231–236.
955 https://doi.org/10.1021/acs.estlett.0c00949

956 Rødland, E., Lin, Y., 2023. Actions Are Needed to Deal with the High Uncertainties in Tire
957 Wear Particle Analyses. Environ. Sci. Technol. 57, 8461–8462.
958 https://doi.org/10.1021/acs.est.3c02393

959 Rødland, E.S., Heier, L.S., Lind, O.C., Meland, S., 2023. High levels of tire wear particles in
960 soils along low traffic roads. Sci. Total Environ. 903, 166470.
961 https://doi.org/10.1016/j.scitotenv.2023.166470

962 Rødland, E.S., Samanipour, S., Rauert, C., Okoffo, E.D., Reid, M.J., Heier, L.S., Lind, O.C.,
963 Thomas, K.V., Meland, S., 2022. A novel method for the quantification of tire and polymer-
964 modified bitumen particles in environmental samples by pyrolysis gas chromatography mass
965 spectroscopy. J. Hazard. Mater. 423, 127092. https://doi.org/10.1016/j.jhazmat.2021.127092

966 Roubeau Dumont, E., Gao, X., Zheng, J., Macairan, J., Hernandez, L.M., Baesu, A., Bayen, S.,
967 Robinson, S.A., Ghoshal, S., Tufenkji, N., 2023. Unraveling the toxicity of tire wear
968 contamination in three freshwater species: From chemical mixture to nanoparticles. J. Hazard.
969 Mater. 453, 131402. https://doi.org/10.1016/j.jhazmat.2023.131402

970 Sebastia, J., Van Oort, F., Lamy, I., 2008. Buffer capacity and Cu affinity of soil particulate
971 organic matter (POM) size fractions. Eur. J. Soil Sci. 59, 304–314.
972 https://doi.org/10.1111/j.1365-2389.2007.01001.x

973 Shi, J., Wu, Q., Zheng, C., Yang, J., 2018. The interaction between particulate organic matter
974 and copper, zinc in paddy soil. Environ. Pollut. 243, 1394–1402.
975 https://doi.org/10.1016/j.envpol.2018.09.085

Smyth, K., Drake, J., Li, Y., Rochman, C., Van Seters, T., Passeport, E., 2021. Bioretention cells remove microplastics from urban stormwater. Water Research 191, 116785. https://doi.org/10.1016/j.watres.2020.116785

Sommer, F., Dietze, V., Baum, A., Sauer, J., Gilge, S., Maschowski, C., Gieré, R., 2018. Tire Abrasion as a Major Source of Microplastics in the Environment. Aerosol Air Qual. Res. 18, 2014–2028. https://doi.org/10.4209/aaqr.2018.03.0099

Sun, B., Li, J., Xiang, L., Lin, F., Che, L., Tian, W., Yan, B., Chen, G., 2022. Simulating vulcanization process during tire production to explore sulfur migration during pyrolysis. Fuel 330, 125665. https://doi.org/10.1016/j.fuel.2022.125665

Tedoldi, D., Charafeddine, R., Branchu, P., Thomas, E., Gromaire, M.-C., 2021. Intra- and inter-site variability of soil contamination in road shoulders – Implications for maintenance operations. Sci. Total Environ. 769, 144862. https://doi.org/10.1016/j.scitotenv.2020.144862

Tedoldi, D., Chebbo, G., Pierlot, D., Branchu, P., Kovacs, Y., Gromaire, M.-C., 2017. Spatial distribution of heavy metals in the surface soil of source-control stormwater infiltration devices – Inter-site comparison. Sci. Total Environ. 579, 881–892. https://doi.org/10.1016/j.scitotenv.2016.10.226

Thorpe, A., Harrison, R.M., 2008. Sources and properties of non-exhaust particulate matter from road traffic: A review. Sci. Total Environ. 400, 270–282. https://doi.org/10.1016/j.scitotenv.2008.06.007

995 Tian, Z., Zhao, H., Peter, K.T., Gonzalez, M., Wetzel, J., Wu, C., Hu, X., Prat, J., Mudrock, E.,
996 Hettinger, R., Cortina, A.E., Biswas, R.G., Kock, F.V.C., Soong, R., Jenne, A., Du, B., Hou,
997 F., He, H., Lundeen, R., Gilbreath, A., Sutton, R., Scholz, N.L., Davis, J.W., Dodd, M.C.,
998 Simpson, A., McIntyre, J.K., Kolodziej, E.P., 2021. A ubiquitous tire rubber–derived chemical
999 induces acute mortality in coho salmon. Science 371, 185–189.
1000 https://doi.org/10.1126/science.abd6951

1001 Turner, A., Filella, M., 2023. Lead and chromium in European road paints. Environ. Pollut.
1002 316, 120492. https://doi.org/10.1016/j.envpol.2022.120492

1003 Unice, K.M., Kreider, M.L., Panko, J.M., 2013. Comparison of Tire and Road Wear Particle
1004 Concentrations in Sediment for Watersheds in France, Japan, and the United States by
1005 Quantitative Pyrolysis GC/MS Analysis. Environ. Sci. Technol. 47, 8138–8147.
1006 https://doi.org/10.1021/es400871j

1007 Unice, K.M., Kreider, M.L., Panko, J.M., 2012. Use of a Deuterated Internal Standard with
1008 Pyrolysis-GC/MS Dimeric Marker Analysis to Quantify Tire Tread Particles in the
1009 Environment. Int. J. Environ. Res. Public. Health 9, 4033–4055.
1010 https://doi.org/10.3390/ijerph9114033

1011 U.S. Environmental Protection Agency, 2021. Stormwater Best Management Practice -
1012 Infiltration Basin [PDF document]. https://www.epa.gov/system/files/documents/2021-
1013 11/bmp-infiltration-basin.pdf (accessed 09.10.24).

1014 Wagner, S., Klöckner, P., Reemtsma, T., 2022. Aging of tire and road wear particles in
1015 terrestrial and freshwater environments – A review on processes, testing, analysis and impact.
1016 Chemosphere 288, 132467. https://doi.org/10.1016/j.chemosphere.2021.132467

Wei, H., Flanagan, K., Lundy, L., Muthanna, T.M., Viklander, M., 2023. A study of 101 organic substances in gully pot sediments accumulated over a one-year period in Stockholm, Sweden. Sci. Total Environ. 894, 165028. https://doi.org/10.1016/j.scitotenv.2023.165028

Werbowski, L.M., Gilbreath, A.N., Munno, K., Zhu, X., Grbic, J., Wu, T., Sutton, R., Sedlak, M.D., Deshpande, A.D., Rochman, C.M., 2021. Urban Stormwater Runoff: A Major Pathway for Anthropogenic Particles, Black Rubbery Fragments, and Other Types of Microplastics to Urban Receiving Waters. ACS EST Water 1, 1420–1428. https://doi.org/10.1021/acsestwater.1c00017

Yang, K., Jing, S., Liu, Yang, Zhou, H., Liu, Yan, Yan, M., Yi, X., Liu, R., 2022. Acute toxicity of tire wear particles, leachates and toxicity identification evaluation of leachates to the marine copepod, Tigriopus japonicus. Chemosphere 297, 134099. https://doi.org/10.1016/j.chemosphere.2022.134099

Zannoni, D., Valotto, G., Visin, F., Rampazzo, G., 2016. Sources and distribution of tracer elements in road dust: The Venice mainland case of study. J. Geochem. Explor. 166, 64–72. https://doi.org/10.1016/j.gexplo.2016.04.007

Zhu, J., Guo, R., Ren, F., Jiang, S., Jin, H., 2024. Occurrence and partitioning of *p*-phenylenediamine antioxidants and their quinone derivatives in water and sediment. Sci. Total Environ. 914, 170046. https://doi.org/10.1016/j.scitotenv.2024.170046

Ziajahromi, S., Lu, H.-C., Drapper, D., Hornbuckle, A., Leusch, F.D.L., 2023. Microplastics and Tire Wear Particles in Urban Stormwater: Abundance, Characteristics, and Potential Mitigation Strategies. Environ. Sci. Technol. 57, 12829–12837. https://doi.org/10.1021/acs.est.3c03949